GEOPHYSICAL RESEARCH LETTERS, VOL. 18, NO. 12, PAGES 2201-2204, DECEMBER 1991

WAVEFORM EFFECTS OF A METASTABLE OLIVINE TONGUE IN SUBDUCTING SLABS

John E. Vidale

United States Geological Survey, Menlo Park, California

Quentin Williams and Heidi Houston

Earth Sciences Dept. and Institute of Tectonics, University of California, Santa Cruz

Abstract. We constructed velocity models of subducting slabs with a kinetically-depressed olivine --> β- and γ-spinel transition, and examined the effect that such structures would have on teleseismic P waveforms using a full-wave finite-difference method. These two-dimensional calculations yielded waveforms at a range of distances in the downdip direction. The slab models included a wedge-shaped, low-velocity metastable olivine tongue (MOTO) to a depth of 670 km, as well as a plausible thermal anomaly; one model further included a 10-km-thick fast layer on the surface of the slab. The principal effect of MOTO is to produce grazing reflections at wide angles off the phase boundary, generating a secondary arrival 0 to 4 seconds after the initial arrival depending on the take-off angle. The amplitude and timing of this feature vary with the lateral location of the seismic source within the slab cross-section. Careful analysis of waveforms from earthquakes with depths near 400 km, simple sources, and adequate station coverage in appropriate geometries will be required to resolve whether MOTO is present.

Introduction

The Earth's mantle undergoes a major seismic and mineralogic change at about 400 km depth as silicate olivine transforms to the higher-pressure β-phase. This paper is concerned with this discontinuity as it occurs in cold subducting slabs. Although colder temperatures within slabs are thought to elevate the equilibrium boundary of the olivine to β-phase transition due to the positive Clapeyron slope of this reaction [*Solomon and U*, 1975; *Roecker*, 1985; *Helffrich et al.*, 1989], low temperatures could instead kinetically impede the reaction, thus depressing this boundary within the core of the slab [*Sung*, 1979; *Sung and Burns*, 1976]. Thus, a wedge-shaped region of metastable olivine may persist in subducted lithosphere to depths well below 400 km. Such a feature would form a relatively low-velocity and low-density channel within the slab that would act as a seismic waveguide. This low-velocity structure might be difficult to observe by arrival time tomography, since the first arriving seismic waves tend to stay in fast material [*Iidaka and Suegetsu*, 1990]. Here, we investigate the effects on teleseismically-recorded compressional (P) waveforms of a metastable olivine tongue (MOTO) extending from 400 km to 670 km in order to evaluate the prospects for resolving the presence of such a structure.

The geophysical consequences of such a feature are profound. It has been suggested that deep earthquakes are caused by a shear instability associated with the transformation of metastable olivine to its high-pressure phases (β, with a spinelloid structure and γ, with the spinel structure) in the slab under deviatoric stresses [*Burnley et al.*, 1991; *Kirby et al.*, 1991; *Green et al.*, 1991]. Furthermore, if MOTO is present, then both the buoyancy forces and the stress state in the deep slab would differ from those produced by simple elevation of the phase boundary [e.g., *Goto et al.*, 1987]. Thus, the presence or absence of MOTO has important implications for slab structure, the dynamics of the subduction process, and the physical mechanism by which deep earthquakes occur. Nevertheless, the present work is the first effort to examine the possible teleseismic signature of metastable olivine within subducting slabs.

Slab Velocity Model

The general slab velocity structure for which we compute waveforms is shown in Figure 1. We assumed a slab dip of 50°, and took the dimensions of MOTO as approximately equivalent to those defined by the 900°C slab isotherm in the calculations of *Schubert et al.* [1975] (ignoring the latent heat of transformation produced by phase transitions). This isotherm corresponds to the kinetic estimate of *Sung* [1979] for the minimum transition temperature from $(Mg_{0.9}Fe_{0.1})_2SiO_4$-olivine to spinel within the slab, assuming an activation volume for the transition of ~10 cm^3/mole. The kinetics of the transition to the β-phase are likely to be either similar to, or less rapid than those to the γ-phase [*Rubie and Brearley*, 1991]. Moreover, this isotherm spans the depth range over which deep earthquakes occur. Therefore, if transforming metastable olivine does produce all earthquakes from 400 to 670 kilometers in depth [e.g. *Burnley et al.*, 1991; *Kirby et al.*, 1991], then a low-velocity feature with about the length shown in Figure 1 must be present within the slab.

We assume a 5% contrast in P-wave velocity across the phase boundary within the slab. This corresponds to an olivine abundance of about 60% within the slab at 400 km depth, and is consistent with estimates of the P-wave velocity

Model of metastable olivine tongue (MOTO) in subducting slab

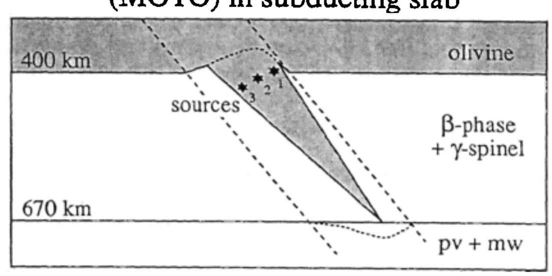

Fig. 1. Schematic of slab model with low-velocity metastable olivine tongue (MOTO) within the subducting slab. Velocity contrast across the olivine --> β-phase + γ-spinel boundary is assumed to be 5%; the width of the low-velocity wedge is 70 km at 400 km depth. Stars show different source locations used to compute waveforms. Approximate locations of the equilibrium phase transitions from olivine to the β-phase, and from γ-spinel to perovskite and magnesiowüstite (pv+mw) are shown by dotted lines. Dashed lines indicate the extent of the slab thermal anomaly.

Paper number 91GL02588
0094-8534/91/91GL-02588$03.00

contrast across the 400 km discontinuity in ambient mantle [*LeFevre and Helmberger*, 1989]. The velocity discontinuity across the transition is assumed to be sharp: *Sung* [1979] has estimated that this transition will proceed from 10 to 90% completion across about a 50°C interval in temperature. In the slab thermal model of *Schubert et al.* [1975], this corresponds to a thickness of the transition of less than ~7 kilometers. Thus, relative to its overall dimension and the wavelengths of the seismic waves, the boundaries of the feature are likely to be relatively sharp. However, we note the possibility that regions of metastable olivine may be heterogeneously distributed in the subducting slab, with non-planar boundaries between the olivine and spinel phases [*Frohlich*, 1987].

Our model also includes an elevation of the olivine to β–phase transition in the higher temperature, non-kinetically impeded regions of the slab by approximately 25 kilometers. This is based upon a Clapeyron slope for this transition of ~1.5 x 10^{-3} GPa/°C [*Akaogi et al.*, 1989], and an assumed temperature difference between the kinetic boundary and the ambient mantle of ~500°C at 400 kilometers depth [*Sung*, 1979; *Helffrich et al.*, 1989; *Akaogi et al.*, 1989]. The 670 km depth discontinuity may also be displaced due to the thermal anomaly associated with the slab, but this feature would not produce a significant effect on the calculated waveforms and is not included in our velocity models.

All our models incorporate the longer wavelength thermal perturbation in velocity structure thought to be associated with the slab. Specifically, we assume -0.4 m/sec/°C for the derivative of the compressional velocity with respect to temperature (dV_p/dT) [e.g. *Anderson*, 1987]. We also assume a maximum temperature change of approximately 800°C, with a width of 200 km based on the estimated locations of isotherms within the slab [*Schubert et al.*, 1975; *Helffrich et al.*, 1989]. The resulting velocity anomaly is 3.5% fast near the upper surface of the slab, and drops off linearly to 0% anomaly both 30 km normal to the slab above and 170 km below the maximum velocity (e.g., the cold core of the slab). All models also include the normal increases of seismic velocity with depth.

The final structural element tested in our simulations is a 10-km-thick layer on the upper surface of the slab with a velocity 5% higher than ambient mantle; we extend this layer to a depth of 1000 km. Such a structure has been invoked to explain early arrivals in New Zealand from events in Tonga [*Ansell and Gubbins*, 1986].

Results

Compressional waveforms were computed using the two-dimensional, fourth-order finite difference method of *Vidale* [1990] with an isotropic source. The full-wave finite difference scheme is used to propagate seismic waves through the slab model; a Kirchhoff method is then used to extrapolate the waves to teleseismic distances [*Stead and Helmberger*, 1988]. The two-dimensional simulations yield an accurate approximation in the downdip direction. Conversions of shear to compressional waves are ignored in our acoustic wave simulations; the inclusion of such conversions would mainly serve to further complicate the later part of the waveform.

Waveforms were computed for take-off angles at approximately 4° increments above and below the dip of the slab. For a slab that dips 50° (recall that dip is measured from the horizontal and take-off angle from the vertical), take-off angles from 50° to 20° span the distance range of 30° to 90°. This geometry resembles paths from the Kurile slab to European stations. Subduction zones that dip more or less than 50° will show a similar pattern of waveform effects shifted to greater or smaller distances, respectively.

Seismic sources are placed at depths near 400 km, as this is the source depth at which waveforms will be most strongly affected by MOTO, because the seismic waves can travel the entire length of the structure. As expected, simulations with a source at 580 km depth showed much less effect of the MOTO structure on waveforms than those with sources near 400 km.

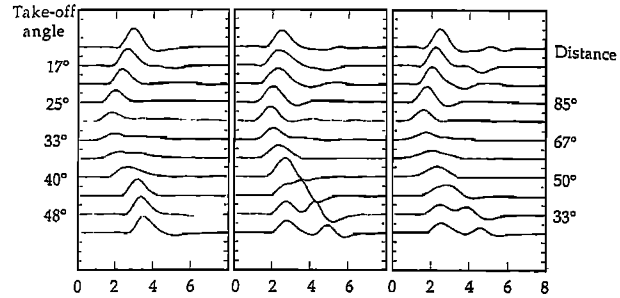

Fig. 2. Teleseismic P waveforms from a source at location 1 (see Figure 1) for slab models including: (a) only a thermal anomaly of 3.5%, (b) the thermal anomaly and the MOTO structure as shown in Figure 1, and (c) the thermal anomaly, the MOTO structure, and a high-velocity (5% fast) 10-km-thick layer on the surface of the slab.

Figure 2 is a comparison of waveforms generated by different slab structures with a source at 400 km depth near the upper surface of the slab (location 1 in Figure 1). The primary effect of the thermal anomaly (Figure 2a) is to broaden and reduce the amplitude of the waveforms for take-off angles near the dip of the slab (at distances between 50° and 75° for a slab dipping 50°); see *Vidale* [1987] for further discussion of the effect of various thermal anomalies on waveforms. When the MOTO structure is included (Figure 2b), the effect of the thermal structure is partially counteracted.

More significantly, however, the presence of MOTO introduces grazing reflections at wide angles off the sharp phase boundary. Depending on the take-off angle, these reflections can generate a secondary arrival 0 to 3 seconds after the first arrival. The strong secondary arrival at shallow take-off angles in Figure 2b is the reflection off the lower edge of MOTO. At steep take-off angles, the secondary arrival is not a geometric ray, but a diffraction. The first arrival consists of energy that has traveled a shorter distance in the low-velocity metastable olivine than later arrivals. The MOTO structure has an effect intermediate between a lens and a waveguide, channeling and delaying some of the energy. Because the width of the thermal anomaly is large relative to that of MOTO, the secondary arrivals produced by MOTO are not strongly affected by the amplitude of the thermal anomaly. Similarly, because of its small length scale, the effect of a 10-km-thick, fast lid near the upper surface of the slab is not large (Figure 2c). This structure accentuates the small secondary arrival at take-off angles below the slab (large distances), and depletes the high frequencies at take-off angles above the slab (small distances).

Results of simulations including the simplest MOTO structure and the thermal anomaly, with sources located at points 1, 2, and 3 in Figure 1, are shown in Figures 3a, b, and c, respectively. All three sources give rise to secondary arrivals produced by grazing reflections off the olivine-spinel boundary. The amplitude and timing of these secondary arrivals depend on the lateral location of the source within the slab cross-section, as well as the take-off angle. This strong dependence of the waveforms on source location will introduce some uncertainty into the interpretation of actual waveforms, as the precise locations of deep earthquakes are presently poorly known.

If the olivine --> β- or γ-spinel transitions have positive activation volumes, then at greater depths, the temperature at which the transformation occurs in the slab would increase [*Sung*, 1979]. Thus, the boundaries of MOTO may be

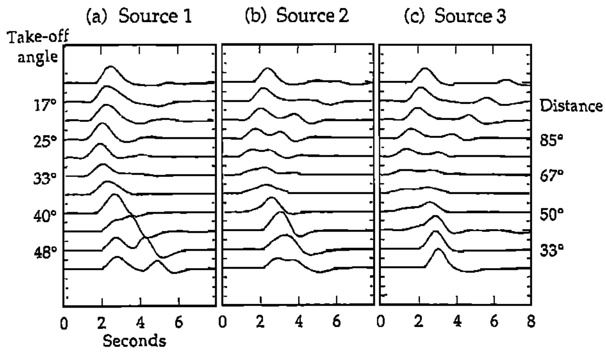

Fig. 3. Teleseismic P waveforms from sources at different locations in a slab with the MOTO structure. The sources for (a), (b), and (c) are at points 1, 2, and 3, respectively, in Figure 1.

broader than a given isotherm at depth within the slab, increasing the region of olivine metastability, and producing a broader, blunter structure than is shown in Figure 1. Simulations with a slab model incorporating a broadened, rounded MOTO indicate that the effect on waveforms is not significantly different from that of a wedge-shaped structure.

Taken together, our simulations document that a structure similar to MOTO will produce prominent waveform complexity in the form of secondary arrivals at some take-off angles regardless of the location of a 400 km deep source within the slab. This complexity is present for all the velocity structures that we tested and for various amplitudes of the slab thermal anomaly. Shear waveforms may exhibit somewhat greater complexity than compressional waveforms; however, since shear waves are more attenuated, the complications would probably be more difficult to resolve.

Some effects of the MOTO structure on the waveforms can be fairly subtle; for example, rise times (the time from initial arrival to peak amplitude) of P-waveforms of events near 400 km depth are either unchanged or lengthened by MOTO. Therefore, observations of deep (>450 km) earthquakes with rise times almost twice as fast as those of shallower slab events cannot be explained by the MOTO velocity structure [*Houston and Williams*, 1991]; in fact, this structure would be most likely to increase the observed rise times of deep events.

Discussion

As demonstrated by our simulations, teleseismic waveforms represent a promising approach for resolving the presence of a low-velocity metastable olivine wedge in subducting slabs. This approach, however, may be hampered by several factors intrinsic to the nature and geometry of MOTO. First, as shown by Figure 3, uncertainty in the lateral location of the source can introduce ambiguity into the interpretation of data. Also, the source depth, 400 km, at which waveforms would be most strongly affected by MOTO corresponds closely to a minimum in deep seismicity [*Frohlich*, 1989]. Since the effects of MOTO on sources significantly deeper than about 500 km are small, there are few large, impulsive events that have the potential to show strong effects from MOTO. Moreover, about half of all deep earthquakes have complex source time functions, with multiple sub-events [e.g. *Fukao and Kikuchi*, 1987; *Frohlich*, 1989; *Houston and Williams*, 1991]. Such source complexity can further complicate the interpretation of waveform effects of the type shown in Figures 2 and 3. Furthermore, at distances greater than about 75°, core and core-mantle-boundary related phases may interfere with secondary arrivals produced by MOTO [e.g. *Weber and Davis*, 1990]. Finally, there is only a limited amount of broadband teleseismic data collected in an appropriate geometry with sufficiently dense station coverage. However, none of these problems preclude using teleseismic waveforms to resolve whether MOTO is present.

If metastable olivine exists within the slab, it may be present in structures more complex than the simple structures modeled here. Such structures might have irregular boundaries or regions converted to spinel distributed heterogeneously throughout the wedge [e.g. *Frohlich*, 1987]. The effects of a more complicated structure are difficult to predict. We expect that greater structural complexity with scale lengths of 5 to 50 km would produce more waveform complexity; however, it may also deplete higher frequencies. Increased waveform complexity may facilitate the identification of metastable olivine, whereas depletion of higher frequencies may hinder it.

Conclusions

This study provides one means by which the presence of a low-velocity metastable olivine wedge within a subducting slab could be seismically resolved. Although the details of the waveforms depend on source location within the slab, our simulations document that MOTO structures similar to those modeled here will generate significant waveform complexity, primarily in the form of secondary arrivals 0 to 4 seconds after the initial P wave for events near 400 km depth. Teleseismic waveforms represent a promising mechanism with which to examine such a feature, although some difficulties may arise in practice. These include uncertainty in source location, a paucity of earthquakes near 400 km depth, earthquake source complexity, limited broadband teleseismic data with the appropriate geometry, and interference from core-related phases.

Acknowledgements: We thank T. Lay, E. Knittle, S. Grand, S. Kirby, and H. Benz for helpful comments. Contribution #140 of the Institute of Tectonics (C.F. Richter Seismological and Mineral Physics Laboratories). This work was partially supported by NASA (Q.W.), NSF (H.H.) and the W.M. Keck Foundation.

References

Akaogi, M., E. Ito and A. Navrotsky, Olivine-modified spinel-spinel transitions in the system Mg_2SiO_4-Fe_2SiO_4: Calorimetric measurements, thermochemical calculations, and geophysical applications, *J. Geophys. Res., 94,* 15,671-15,688, 1989.

Anderson, D.L., Thermally induced phase changes, lateral heterogeneity of the mantle, continental roots, and deep slab anomalies, *J. Geophys. Res., 92,* 13968-13980, 1987.

Ansell, J.H., and D. Gubbins, Anomalous high-frequency wave propagation from the Tonga-Kermadec seismic zone to New Zealand, *Geophys. J. R. Astr. Soc., 85,* 93-106, 1986.

Burnley, P.C., H.W. Green II and D.J. Prior, Faulting associated with the olivine to spinel transformation in Mg_2GeO_4 and its implications for deep-focus earthquakes, *J. Geophys. Res., 96,* 425-443, 1991.

Frohlich, C., Aftershocks and temporal clustering of deep earthquakes, *J. Geophys. Res., 92,* 13944-13956, 1987.

Frohlich, C., The nature of deep-focus earthquakes, *Ann. Rev. Earth Planet. Sci., 17,* 227-254, 1989.

Fukao, Y., and M. Kikuchi, Source retrieval for mantle earthquakes by iterative deconvolution of long-period P waves, *Tectonophysics, 144,* 249-269, 1987.

Goto, K., Z. Suzuki, and H. Hamaguchi, Stress distribution due to olivine-spinel phase transition in descending plate and deep focus earthquakes, *J. Geophys. Res., 92,* 13,811-13,820, 1987.

Green, H.W., T.E. Young, D. Walker and C.H. Scholz, Anticrack-associated faulting at very high pressure in natural olivine, *Nature, 348,* 720-722, 1990.
Helffrich, G.R., S. Stein, and B.J. Wood, Subduction zone thermal structure and mineralogy and their relationship to seismic wave reflections and conversions at the slab/mantle interface, *J. Geophys. Res., 94,* 753-763, 1989.
Houston, H., and Q. Williams, Fast rise times and the physical mechanism of deep earthquakes, *Nature, 352,* 520-522, 1991.
Iidaka, T., and D. Suegetsu, A travel time analysis for the olivine-spinel phase boundary inside the subducting slab, *EOS, 71,* 1574-1575, 1990 (abstract).
Kirby, S.H., W.B. Durham, and L.A. Stern, Phase transformations, anomalous faulting and deep earthquakes: A new perspective, *Science, 252,* 216-225, 1991.
LeFevre, L.V., and D.V. Helmberger, Upper mantle P velocity structure of the Canadian shield, *J. Geophys. Res., 94,* 17,749-17,765, 1989.
Roecker, S.W., Velocity structure in the Izu-Bonin seismic zone and the depth of the olivine-spinel phase transition in the slab, *J. Geophys. Res., 90,* 7771-7794, 1985.
Rubie, D.C. and A.J. Brearley, Mechanism of the γ–β phase transformation of Mg_2SiO_4 at high temperature and pressure, *Nature, 348,* 628-631, 1990.
Schubert, G., D.A. Yuen and D.L. Turcotte, Role of phase transitions in a dynamic mantle, *Geophys. J. R. Astr. Soc., 42,* 705-735, 1975.
Solomon, S.C., and K.T.P. U, Elevation of the olivine-spinel transition in subducted lithosphere: Seismic evidence, *Phys. Earth Planet. Inter., 11,* 97-108, 1975.
Stead, R.J., and D.V. Helmberger, Numerical-analytical interfacing in two dimensions with applications to modeling NTS seismograms, *Pure Appl. Geophys., 128,* 157-193, 1988.
Sung, C.M., Kinetics of the olivine-spinel transition under high pressure and temperature: Experimental results and geophysical implications, in *High-Pressure Science and Technology,* K.D. Timmerhaus and M.S. Barber (Eds.), pp. 31-41, Plenum, N.Y., 1979.
Sung C.M. and R.G. Burns, Kinetics of the olivine-spinel transition: Implications to deep-focus earthquake genesis, *Earth Planet. Sci. Lett., 32,* 165-170, 1976.
Vidale, J., Waveform effects of a high-velocity, subducted slab, *Geophys. Res. Letts., 14,* 542-545, 1987.
Vidale, J., Comment on "A comparison of finite-difference and Fourier method calculations of synthetic seismograms" by C.R. Daudt et al., *Bull. Seism. Soc. Am., 80,* 493-495, 1990.
Weber, M, and J.P. Davis, Evidence of a laterally variable lower mantle structure from P and S waves, *Geophys. J. Int., 102,* 231-255, 1990.
Zhou, H.W., and R.W. Clayton, P and S wave travel time inversions for subducting slab under the island arcs of the Northwest Pacific, *J. Geophys. Res., 95,* 6829-6851, 1990.

J. Vidale, US Geological Survey, 345 Middlefield Road, Menlo Park, CA 94025.
Q. Williams and H. Houston, Earth Sciences Dept., University of California, Santa Cruz, CA 95064.

(Received August 23, 1991;
accepted October 9, 1991.)